Anomalous Second-Order Nonlinear Optical Response of In-Plane Poled Glassy Polymers. Spectroscopic and Theoretical Support for the Importance of Charged Chromophore Aggregates

Shlomo Yitzchaik,*,† Santo Di Bella,*,‡ Paul M. Lundquist,§,|| George K. Wong,§ and Tobin J. Marks*,§

Contribution from the Department of Inorganic and Analytical Chemistry, The Hebrew University of Jerusalem, Jerusalem 91904, Israel, Department of Chemistry, Università di Catania, Catania 95125, Italy, and Department of Chemistry, Department of Physics and Astronomy, and the Materials Research Center, Northwestern University, Evanston, Illinois 60208-3113

Received October 7, 1996[⊗]

Abstract: We report here measurements of the orientational and frequency dependence of the anomalously large second-order nonlinear optical (NLO) susceptibilities observed in guest−host DANS [4-(*N*,*N*-dimethylamino)-4′-nitrostilbene]/PMMA [poly(methyl methacrylate)] films poled in an "in-plane" electrode configuration. The resonant response is sharply peaked (fwhm decreases by a factor of 4) in comparison to identical samples poled by standard corona field techniques. Additionally, these anomalous susceptibilities, which are oriented *normal* to the electric poling field, exhibit unusually strong features at long wavelengths where the linear absorption is low. We also report the first direct experimental EPR evidence for nitrogen-centered cation radicals, hence the creation of charged chromophores trapped in the polymeric matrix by charge injection from the poling electrodes. These observations are in qualitative agreement with the very large NLO response magnitudes and distinct spectral features predicted by sum-over-states perturbative calculations performed for positively charged centrosymmetric chromophore dimers and provide strong computational evidence that the observed anomalous NLO response is due to charged chromophore aggregates.

Chromophore-containing glassy polymers having macroscopic noncentrosymmetry induced by electric field poling are among the most promising materials identified to date for second-order thin film nonlinear optical (NLO) applications.[1] They are of great scientific and technological interest because of the large NLO response (e.g., second harmonic generation, SHG, electro-optic response), chemical flexibility, and the inexpensive, straightforward, and efficient fabrication techniques which are applicable.[2,3] The origin of second-order NLO response in poled glassy polymers is generally considered to arise from isolated, hyperpolarizable constituent chromophore molecules and is dominated by electric dipole transitions along the chromophore charge transfer axes which are macroscopically aligned by the poling field. The preferential alignment of the chromophore ground state dipole moments, μ, along the poling field, E_p, direction gives rise to four nonvanishing components of the nonlinear bulk susceptibility, $\chi^{(2)}_{ijk}$, in the weak field limit[2b] (eqs 1 and 2), where N is the chromophore number density, β_{zzz} is

$$\chi^{(2)}_{zzz} = N\beta_{zzz}\frac{\mu_z E_p}{5kT} f^{\omega} f^{\omega} f^{2\omega} \quad (1)$$

$$\chi^{(2)}_{zxx} = \chi^{(2)}_{xzx} = \chi^{(2)}_{xxz} = N\beta_{zzz}\frac{\mu_z E_p}{15kT} f^{\omega} f^{\omega} f^{2\omega} \quad (2)$$

the largest molecular hyperpolarizability tensor component, f's are local field factors, and z is the direction of the poling field, E_p. Adherence to this "chromophore gas" model has been observed consistently in experiments involving electric fields applied normal to the surface of thin film samples poled using corona[1] or contact (sandwich) techniques[4] with high work function electrodes (Figure 1). Although the chromophore gas model adequately explains the vast majority of conventional corona and contact poling results, it cannot explain the results of experiments performed on polymer−chromophore films with poling fields directed within the film using coplanar *in-plane* electrodes.[5] These experiments are performed using relatively weak dc fields but high voltages. The most striking discrepancy between the aligned dipole model and the in-plane results is

† The Hebrew University of Jerusalem.
‡ Università di Catania.
§ Northwestern University.
|| Current address: IBM Research Division, Almaden Research Center, Department K13-D2, 650 Harry Road, San Jose, CA 95120-6099.

⊗ Abstract published in *Advance ACS Abstracts,* December 15, 1996.

(1) (a) Marks, T. J.; Ratner, M. A. *Angew. Chem., Int. Ed. Eng.* **1995**, *7*, 426. (b) Burland, D. M.; Miller, R. D.; Walsh, C. A. *Chem. Rev.* **1994**, *94*, 31. (c) Marder, S. R.; Perry, J. W. *Adv. Mater.* **1993**, *11*, 804.

(2) (a) Lindsay, G. A., Singer, K. D., Eds. *Polymers for Second-Order Nonlinear Optics*; ACS Symposium Series 601; American Chemical Society: Washington, DC, 1995. (b) Zyss, J., Ed. *Molecular Nonlinear Optics*; Academic Press: San Diego, CA, 1994. (c) Zyss, J., Ed. *Molecular Nonlinear Optics: Materials, Physics and Devices*; Academic Press: Boston, MA, 1993. (d) Prasad, P. N. *Contemporary Nonlinear Optics*; Academic Press: San Diego, CA, 1992. (e) Prasad, P. N.; Williams, D. J. *Introduction to Nonlinear Optical Effects in Molecules and Polymers*; Wiley: New York, 1991. (f) Marder, S. R., Sohn, J. E., Stucky, G. D., Eds. *Materials for Nonlinear Optics: Chemical Prespective*; ACS Symposium Series 455; American Chemical Society: Washington, DC, 1991. (g) Chemla, D. S., Zyss, J., Eds. *Nonlinear Optical Properties of Organic Molecules and Crystals*; Academic Press: New York, 1987; Vols. 1 and 2.

(3) (a) Dalton, L. R.; Harper, A. W.; Ghosn, R.; Steir, W. H.; Ziari, M.; Fetterman, H.; Shi, Y.; Mutacich, R. V.; Jen, A. K.-Y.; Shea, K. J. *Chem. Mater.* **1995**, *7*, 1060. (b) Burland, D. M., Ed. *Chem. Rev.* **1994**, *94*.

(4) Singer, K. D.; Sohn, J. E.; Lalama, S. L. *Appl. Phys. Lett.* **1986**, *49*, 248.

(5) Yitzchaik, S.; Berkovic, G.; Krongauz, V. *Adv. Mater.* **1990**, *2*, 33.

S0002-7863(96)03489-0 CCC: $14.00

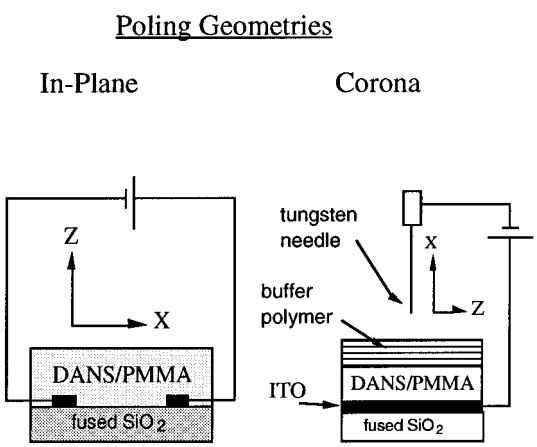

Figure 1. Experimental poling configurations used in this study.

that the largest SHG response in the latter is oriented *perpendicular* to that static poling field vector. It was suggested (but not substantiated) that the large perpendicular $\chi^{(2)}$ response is related to charge injection into the film.[6,7] Evidence for charge injection derives from the observation that the perpendicular response is inhibited in cases of more resistive substrates[8,9] and with higher work function electrodes.[10] It has also been suggested, although not unambiguously confirmed, that the charge injection produces *charged* chromophore aggregates of unknown structure which are responsible for the anomalous perpendicular response.[11] Chromophore aggregates have not generally been considered to be important in poled polymer matrices,[12] and in most cases, eqs 1 and 2 adequately describe the NLO response.[1−3,13] However, the in-plane poling response increases nonlinearly with increasing field strength,[14] fluorescence assignable to chromophore aggregates is detected even at low chromophore concentrations,[15] and charge gradients are detected normal to the dc poling field[16]—all inconsistent with classical behavior.

The purpose of this contribution is to present, using a combination of experimental and semiempirical theoretical techniques, the crucial aspects of what represents a new mechanism for poling-induced polymeric NLO response. For in-plane poled archetypical PMMA [poly(methyl methacrylate)] films doped with DANS [4-(*N*,*N*-dimethylamino)-4′-nitrostilbene], we use EPR to identify nitrogen-centered radicals, showing that charge is indeed injected and trapped on the chromophore molecules. We also investigate the $\chi^{(2)}$ response frequency dependence (dispersion) of "in-plane" poled DANS/PMMA polymer films, showing that it is distinct from the "aligned monomer" response of corona-poled films (which tracks the DANS monomer linear optical spectrum). Moreover, the theoretically predicted frequency response of model DANS charged dimers, evaluated using the INDO/SOS formalism,[17] is shown to agree favorably with the experimental $\chi^{(2)}$ dispersion of the in-plane poled films. In an accompanying contribution,[18] it is demonstrated using more elaborate *ab initio* supermolecular calculations on the archetypical model *p*-nitroaniline cation radical dimer that localized hole states can exhibit large and distinctive static second-order NLO response compared to the neutral PNA monomer. Furthermore, these calculations indicate that the aggregate formation stabilizes the radical cation and enhances the optical nonlinearity. In other words, if charged aggregate formation indeed occurs, it is expected to give rise to a distinctive and far larger (than the monomer) NLO response. Taken together these findings lead us to propose a new model for the strong, anomalous optical nonlinearity normal to the in-plane poling direction.

Experimental Section

The samples studied in the present work were thin films consisting of a poly(methyl methacrylate) (PMMA) *host* (M_w = 80 000; Aldrich, purified by double methanol reprecipitation in from distilled THF) containing the dissolved chromophore *guest* DANS (Kodak) at 2% by weight. For in-plane poling experiments, 50 nm thick aluminum electrodes were vapor deposited 2.0 mm apart onto cleaned glass substrates which were then dip-coated with a 10−20% polymer/chromophore THF solution (the THF was distilled from Na/K alloy) to yield 1−3 nm thick, doped polymer films. In this geometry, an electric potential is applied across the two electrodes, inducing an electric field within the surface plane between the electrodes (Figure 1). An identical 2% DANS/PMMA composition was also deposited (by spin-coating) onto clean ITO (indium−tin-oxide)-coated glass substrates (thickness = 1.4 μm) and then coated with a poly(*p*-hydroxystyrene) (M_w = 22 000; Hoechst-Celanese) buffer layer (thickness = 0.8 μm, from THF solution) for corona-poling experiments. In both geometries, the poling field direction is defined as the *x* axis (Figure 1). Thus, for the in-plane poling samples, the surface normal is taken to be the *z* axis and the *x* and *y* axes lie in the film plane. The corona-poled sample geometry is defined by the *x* axis (parallel to the poling field) oriented normal to the surface with the *z* and *y* axes lying in the film plane. All electric field poling was performed at room temperature.

EPR Experiments. EPR spectra were recorded on a modified Varian E-4 instrument equipped with a quartz finger Dewar for 77 K operation. The spectra were recorded with a 2.0 s time constant at a 9.24 GHz microwave frequency and a 5.0 G modulation amplitude and were scanned at 25 G/min at 77 K. Sample preparation was carried out in the following manner. A 1.6 μm thick 2% DANS/PMMA film was cast on top of an "in-plane" poling electrode, and a 10^4 V/cm dc poling field was applied at room temperature for 30 min. The sample was then quenched in liquid nitrogen with the poling field on. The dc field was then removed, and the fraction of the film between the poling electrodes (see Figure 1) was freeze-fractured and detached from the substrate and metal electrodes. This sample was attached to a quartz rod with vacuum grease and was kept at 77 K until EPR spectra were measured. A control sample was handled in exactly the same manner but without the application of the dc poling field. Spin counting calibration curves were recorded using measured quantities of DPPH (2,2-diphenyl-1-picrylhydrazyl hydrate, Aldrich) dissolved in PMMA. No phase separation or microcrystallite formation was observed for the concentration range 10^{-4}−2.0 wt % DPPH/PMMA films. These film standards were of similar dimensions (thickness and weight), measured with the same quartz rod, and were placed in the same location of the 77 K EPR cavity used for recording the spectra for the poled samples.

(6) Yitzchaik, S.; Berkovic, G.; Krongauz, V. *J. Appl. Phys*. **1991**, *70*, 3949.
(7) Cohen, R.; Berkovic, G.; Yitzchaik, S.; Krongauz, V. *Mol. Cryst. Liq. Cryst*. **1994**, *240*, 169.
(8) Wu, J.; Valley, J.; Erner, S.; Binkley, E.; Kenney, J.; Lipscomb, G.; Lytel, R. *Appl. Phys. Lett*. **1991**, *58*, 225.
(9) Otomo, A.; Stegeman, G. I.; Horsthuis, W. H. G.; Mohlman, G. R. *Appl. Phys. Lett*. **1994**, *65*, 2389.
(10) Cohen, R.; Berkovic, G. *Mol. Cryst. Liq. Cryst*. **1994**, *252*, 87.
(11) Yitzchaik, S.; Berkovic, G.; Krongauz, V. *Nonlinear Opt*. **1993**, *4*, 265.
(12) Hampsch, H. L.; Yang, J.; Wong, G. K.; Torkelson, J. M. *Macromolecules* **1990**, *23*, 3640.
(13) Page, R. H.; Jurich, M. C.; Reck, B.; Sen, A.; Tweig, R. J.; Swalen, J. D.; Bjorkland, G. C.; Wilson, C. G. *J. Opt. B.* **1990**, *7*, 1239.
(14) (a) Yitzchaik, S.; Berkovic, G.; Krongauz, V. *Chem. Mater*. **1990**, *2*, 162. (b) Yitzchaik, S.; Berkovic, G.; Krongauz, V. *Macromolecules* **1990**, *23*, 3539.
(15) Yam, R.; Cohen, R.; Berkovic, G. *Nonlinear Opt*. **1995**, *11*, 311.
(16) Donval, A.; Berkovic, G.; Yilmaz, S.; Bauer-Gogonea, S.; Brinker, W.; Wirges, W.; Bauer, G.; Gerhard-Multhaupt. R. *Opt. Commun*. **1996**, *123*, 195.
(17) Kanis, D. R.; Ratner, M. A.; Marks, T. J. *Chem. Rev*. **1994**, *94*, 195.
(18) DiBella, S.; Lanza, G.; Fragalà, I.; Yitzchaik, S.; Ratner, M. A.; Marks, T. J. *J. Am. Chem. Soc*. **1997**, *119*, 3099 (following paper in this issue).

Linear and Nonlinear Optical Spectroscopy. Optical spectra in the transmission mode were recorded on a Cary 13 spectrophotometer. Emission spectra in the reflection mode were recorded on a PTI 100 fluorophotometer. Determinations of the second-order susceptibilities of in-plane poled samples were performed by in-situ second harmonic generation (SHG) experiments. Detailed polarization-sensitive measurements[19] were performed at the fundamental wavelength of 1.064 μm ($h\omega = 1.17$ eV). An electric potential at 2.0 kV was applied across the in-plane poling electrodes, generating a poling field of $\sim 10^4$ V cm^{-1}. A detailed study of the second-order electric susceptibility tensor was performed by measuring SHG intensities in various polarization geometries. Samples were initially poled for 30 min, after which time the SHG response was found to stabilize and SHG measurements were initiated. The principal components of the second-order electric susceptibility tensor were $\chi^{(2)}_{xxx}$ (parallel to the dc field; within the film plane) and $\chi^{(2)}_{zzz}$ (orthogonal to the dc field; perpendicular to the surface). $\chi^{(2)}_{xxx}$ was measured at normal incidence with the output polarization analyzer parallel to *x*, the poling field direction. SHG measurements on the corona-poled polymer sample were performed by applying a potential of 3.0 kV to a tungsten needle 1.0 cm away from the film surface to produce corona field of $\sim 10^6$ V cm^{-1} (Figure 1). Radiation for the wavelength-dependent measurement of the film SHG response in the various poling geometries was generated with an optical parametric amplifier (OPA) and accompanying instrumentation, as described previously.[20]

Theoretical Methods. The all-valence INDO/S (intermediate neglect of differential overlap) method,[21] in conjunction with the sum-over excited particle-hole-states (SOS) formalism,[22] was employed for electronic structure calculations. Standard parameters and basis functions were used. In the present approach, the open-shell restricted Hartree−Fock (ROHF) formalism was adopted for the $(DANS)_2^{\bullet+}$ dimer, while the closed-shell restricted Hartree−Fock (RHF) formalism was adopted in all other calculations. The monoexcited configuration interaction (MECI) approximation was employed to describe the excited states (singlet states (S) for closed-shell molecules and doublet states (D) for the open-shell $(DANS)_2^{\bullet+}$ dimer). In all calculations, the lowest 160 energy transitions between SCF electronic configurations (300 doublet states generated) were chosen to undergo CI mixing and were included in the SOS procedure. Further theoretical details on the implementation of the ZINDO code for hyperpolarizability calculations on open-shell doublet systems are reported elsewhere.[23] The perturbative SOS formalism allows the description of the frequency-dependent hyperpolarizabilities, and reasonable accuracy in comparison with experiments has been achieved far from resonance for the real part of the second-order hyperpolarizability, $Re[\beta_{ijk}(-2\omega;\omega,\omega)]$.[17,24] A more realistic treatment of the complete $\beta_{ijk}(-2\omega;\omega,\omega)$ *dispersion* requires, in addition, introduction of damping corrections which take into account various spectral broadening processes. The $\beta_{ijk}(-2\omega;\omega,\omega)$ tensor terms are then allowed to be complex (eq 3).[22b] Here, ω is the frequency of the applied electric field, while $\Omega_{ng} = \omega_{ng} + i\Gamma/2$ and $\Omega^*_{ng} = \omega_{ng} - i\Gamma/2$ are the complex and complex conjugate of ω_{ng}, respectively. $h\omega_{ng}$ is the energy difference between the ground state (g) and excited state n, and $\Gamma = \Gamma_n - \Gamma_g$ is a damping parameter. In the present approach, the Γ damping term is treated phenomenologically by using the peak half-width at half-maximum deduced from optical absorption spectrum. Moreover, an average constant term ($\Gamma = 0.3$ eV) is used for all the computed *ng* transitions. A comparison with the experiment is possible through $|\beta_{ijk}|$ (eq 4), where $Re(\beta_{ijk})$ and $Im(\beta_{ijk})$ are the real and imaginary parts of the β_{ijk} tensor terms (eq 3), respectively.

$$\beta_{ijk}(-2\omega;\omega,\omega) = -\frac{e^3}{4\hbar^2}\Bigg[\sum_{n\neq g}\sum_{\substack{n'\neq g\\ n'\neq n}}\Bigg\{(r^j_{gn'}r^i_{n'n}r^k_{gn} + r^k_{gn'}r^i_{n'n}r^j_{gn}) \times \left(\frac{1}{(\Omega_{n'g}-\omega)(\Omega^*_{ng}+\omega)} + \frac{1}{(\Omega^*_{n'g}+\omega)(\Omega_{ng}-\omega)}\right) + (r^i_{gn'}r^j_{n'n}r^k_{gn} + r^i_{gn'}r^k_{n'n}r^j_{gn})\left(\frac{1}{(\Omega^*_{n'g}+2\omega)(\Omega^*_{ng}+\omega)} + \frac{1}{(\Omega_{n'g}-2\omega)(\Omega_{ng}-\omega)}\right) + (r^j_{gn'}r^k_{n'n}r^i_{gn} + r^k_{gn'}r^j_{n'n}r^i_{gn})\left(\frac{1}{(\Omega_{n'g}-\omega)(\Omega_{ng}-2\omega)} + \frac{1}{(\Omega^*_{n'g}+\omega)(\Omega^*_{n'g}+2\omega)}\right)\Bigg\} + 4\sum_{n\neq g}\Bigg\{[r^j_{gn}r^k_{gn}\Delta r^i_n(\omega^2_{ng}-4\omega^2) + r^i_{gn}(r^k_{gn}\Delta r^j_n + r^j_{gn}\Delta r^k_n)(\omega^2_{ng}+2\omega^2)]\frac{1}{(\Omega^2_{ng}-\omega^2)(\Omega^2_{ng}-4\omega^2)}\Bigg\}\Bigg] \quad (3)$$

$$|\beta_{ijk}| = (Re(\beta_{ijk})^2 + Im(\beta_{ijk})^2)^{1/2} \quad (4)$$

Molecular Geometries. The bond-alternating idealized (BAI) geometry was chosen for calculations on the monomeric DANS chromophore.[25] In all the dimeric structures investigated, the molecular geometries were constructed assuming each DANS monomer to be planar. Calculations on the neutral DANS dimer were performed in three different geometrical cofacial arrangements while constraining the interplanar separation (R) to a value typical of molecular π-stacking distances, 3.6 Å (Chart 1). These are the centrosymmetric conformation (**I**), in which the molecular dipoles (μ_x is the principal vector component) are in an antiparallel arrangement; the eclipsed conformation (**II**), in which the molecular dipoles are in a parallel arrangements (**I** and **II** are both H-type aggregates; β_{xxx} for centrosymmetric **I** should be zero); and the slipped conformation (**III**, J-type aggregates), with an arbitrary slip distance (R') of 3.0 Å, corresponding to a tilt angle of 57°. Calculations of $(DANS)_2^{\bullet+}$ were performed in arrangement **I**.

Chart 1. DANS Dimer Structures

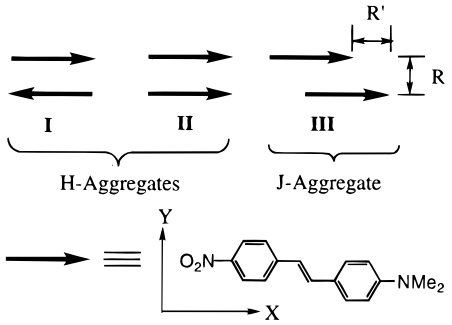

Results

We first report the detection of charged chromophoric species in in-plane poled DANS−PMMA samples which are electronically open shell systems created by charge injection. We then compare the experimental dispersion of the $\chi^{(2)}$ tensor components for the in-plane poled DANS−PMMA samples with DANS−PMMA samples poled using the standard corona-poling technique. Finally, we present theoretical support for a model consistent with centrosymmetric charged dimers being responsible for the anomalous SHG response, by comparing the calculated β_{ijk} dispersion of neutral and charged chromophoric species to the experimental results.

EPR Experiments. The application of high voltage during poling of the DANS-doped polymeric samples creates paramagnetic species with spin Hamiltonian parameters typical of

(19) Lin, W. P.; Lundquist, P. M.; Rippert, E. D.; Ketterson, J. B.; Wong, G. K. *Appl. Phys. Lett.* **1993**, *63*, 2875.
(20) Lundquist, P. M.; Yitzchaik, S.; Zhang, T.; Kanis, D. R.; Ratner, M. A.; Marks, T. J.; Wong, G. K. *Appl. Phys. Lett.* **1994**, *64*, 2194.
(21) (a) Bacon, A. D.; Zerner, M. C. *Theor. Chim. Acta (Berlin)* **1979**, *53*, 21. (b) Ridley, J.; Zerner, M. C. *Theor. Chim. Acta (Berlin)* **1973**, *32*, 111.
(22) (a) Ward, J. F. *Rev. Mod. Phys.* **1965**, *37*, 1. (b) Orr, B. J.; Ward, J. F. *Mol. Phys.* **1971**, *20*, 513.
(23) Di Bella, S.; Fragalà, I.; Marks, T. J.; Ratner, M. A. *J. Am. Chem. Soc.* **1996**, *118*, 12747.
(24) Di Bella, S.; Marks, T. J.; Ratner, M. A. *J. Am. Chem. Soc.* **1994**, *116*, 4440.
(25) Kanis, D. R.; Marks, T. J.; Ratner, M. A. *Int. J. Quantum Chem.* **1992**, *43*, 61.

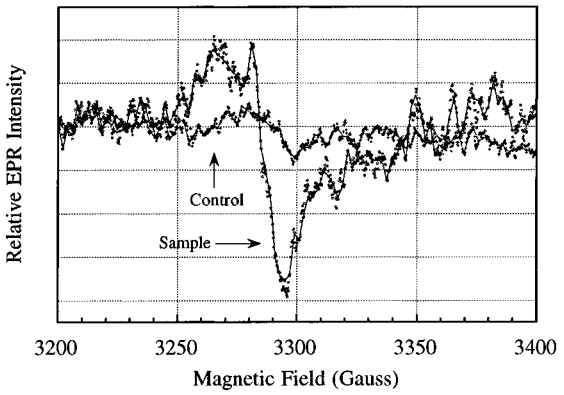

Figure 2. EPR spectrum at 77 K for an in-plane poled 2% DANS + PMMA film sample versus that of an unpoled control sample.

π radical cations. The EPR spectrum of an in-plane poled 2% DANS−PMMA sample (Figure 2) is *ca*. 35 G wide (peak-to-peak) with $g = 2.008 \pm 0.002$. The triplet signal shape and position are characteristic of a nitrogen-centered free radical.[26,27] Due to small sample size and resulting low signal amplitude, it was not possible to unambiguously determine from the hyperfine structure whether the radical is a nitro-centered radical anion or an amine-centered radical cation; however, the observed g value is closer to those of *N*,*N*-dimethylaminobenzene radical cations,[27] rather than to those of nitrobenzene radical anions.[27,28] Other well-characterized aromatic olefinic radical cations, such as *trans*-stilbene derivatives,[29] are characterized by a broader EPR spectrum with $g = 2.0027$.[30] The creation of a stable radical attached to the polymer skeleton, i.e., a carbonyl-centered radical on the ester unit of PMMA, is ruled out since species such as acyl radicals exhibit strong singlets in the EPR with $g = 2.001$.[31]

DPPH, 2,2-diphenyl-1-picrylhydrazyl ($g = 2.0036$), was used as a calibrant to estimate the quantity of radicals produced via spin counting techniques. Double integration of the in-plane poled DANS−PMMA signal intensity DPPH dissolved in PMMA ($1-10^{-4}$ wt %) allowed estimation of the spin number density in the charge-injected sample. The observed signal corresponds to about 10^{13} spins, which represents ~1−2 mol % of the total DANS chromphores dispersed in the film (~10^{-4} weight fraction), in agreement with the number of trapped charges estimated previously from current discharge measurements.[6]

Linear and Nonlinear Optical Response. The linear optical absorption of spectra of corona-poled and in-plane poled DANS-PMMA thin film samples exhibit the same maxima at $\lambda = 433$ nm (Figures 3 and 4, respectively). However, the full width at half-maximum (fwhm) for the corona-poled film is ~100 nm, while that of the in-plane poled sample is ~150 nm and exhibits a pronounced absorption tail extending into the red. Excitation at 380 nm yields a slightly red-shifted emission from the in-plane sample at 595 nm vs 585 nm for the corona-poled sample.

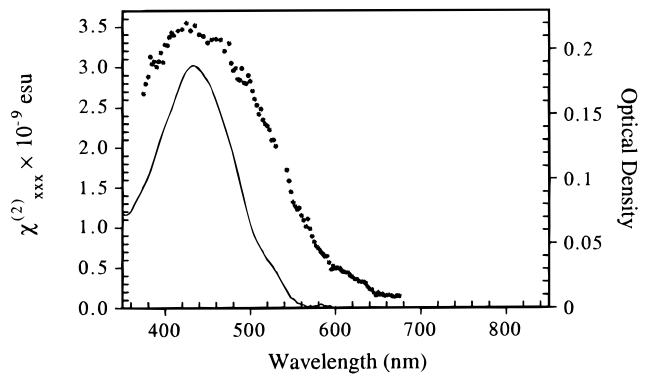

Figure 3. Measured frequency dependence of $\chi^{(2)}_{xxx}$ for a corona-poled 2% DANS + PMMA film as a function of SHG wavelength for incident polarization parallel to the poling field (normal to the film surface plane). The solid line gives the linear absorption.

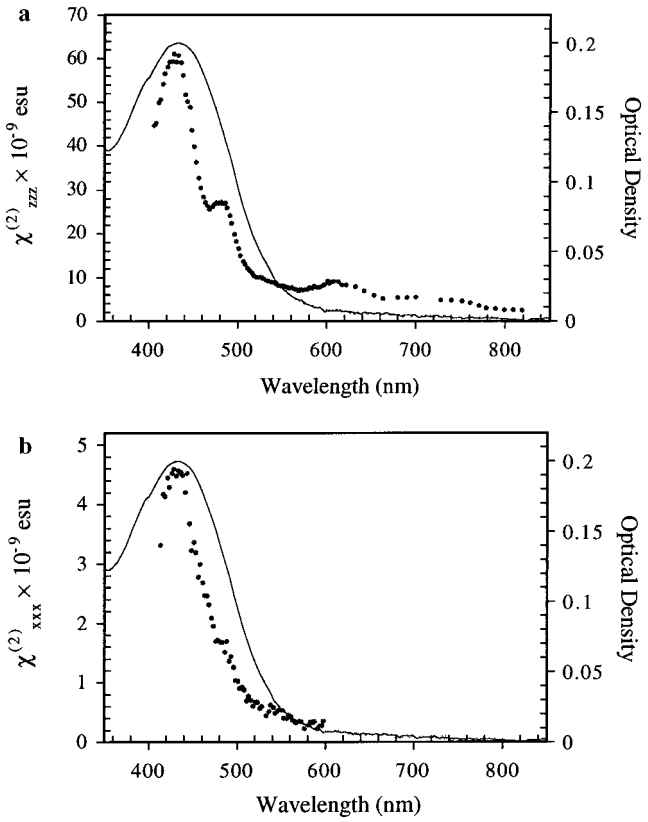

Figure 4. Measured frequency dependence of the second-order optical susceptibility of an in-plane poled 2% DANS + PMMA film as a function of SHG wavelength, along with the linear absorption (solid line): (a) $\chi^{(2)}_{zzz}$ for incident polarization normal to the film surface; (b) $\chi^{(2)}_{xxx}$ for incident polarization parallel to the poling field.

Both samples were measured immediately after the poling field was switched off.

The SHG intensity dependence on the incident polarization was also measured for the in-plane poled sample (Figure 5). The maximum intensity, which occurs for the incident and output polarization parallel to the poling field, was used to compute the magnitude of $\chi^{(2)}_{zzz} = 9 \times 10^{-9}$ esu at the fundamental wavelength of 1.064 μm. The measured value of 4×10^{-10} esu for $\chi^{(2)}_{xxx}$ is in reasonable agreement with that predicted for a DANS-based sample at such a low chromophore number densities and poling fields. Within the chromophore gas picture, the polymeric material should be optically uniaxial, with the symmetry axis directed in the poling field direction (along with vector separating the two electrodes) around which

(26) Ayscough, P. B. *Electron Spin Resonance in Chemistry*; Methuen & Co.: London, 1967; Chapter 8.

(27) (a) Berndt, A.; Neugebauer, F. A. *Magnetic Properties of Free Radicals*; Fischer, H., Ed.; Springer-Verlag: New York, 1987; *Conjugated Carbon and Nitrogen Radicals* (Landolt-Börnstein Tables, Vol. 17, Subvol. c). (b) Fischer, H. *Magnetic Properties of Free Radicals*; In Landolt-Börnstein, New Series, Group II; Hellwege, K.-H., Hellwege, A. M., Eds.; Springer-Verlag: Berlin, 1965.

(28) Rieger, P. H.; Fraenkel, G. K. *J. Chem. Phys.* **1963**, *39*, 609.

(29) Lin, C.-R.; Wang, C.-N.; Ho, T.-I. *J. Org. Chem.* **1991**, *56*, 5025.

(30) Bonazzola, L.; Michaut, J.-P.; Roncin, J.; Misawa, H.; Sakuragi, H.; Takumaru, K. *Bull. Chem. Soc. Jpn.* **1990**, *63*, 347.

(31) Kinell, P.-O.; Rånby, B.; Runnström-Reio, V., Eds. *EPR Applications to Polymer Research—Nobel Symp. 22*; Almqist & Wiksell: Stockholm, 1973.

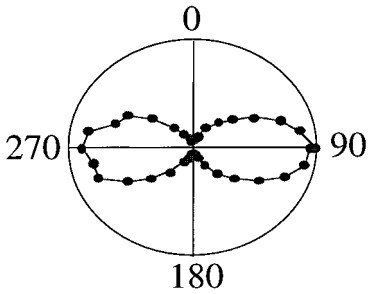

Figure 5. Dependence of the p-polarized SHG intensity of an in-plane poled 2% DANS + PMMA film as a function of the fundamental beam polarization angle at 60° incident angle from the surface normal.

the chromophore axes are distributed uniformly. However, a much larger NLO response (at least 1 order of magnitude) is observed *normal to the film surface*. The magnitude of this $\chi^{(2)}_{zzz}$ was determined by measuring the incident angle dependence of the SHG response in the p−p polarization configuration. In this geometry, zero SHG response is predicted for isolated chromophore molecules; however, extremely large responses are observed for non-zero incident angles and these peak at 60°. In this case, the tensor components that contribute to the SHG response are $\chi^{(2)}_{zzz}$ and $\chi^{(2)}_{zxx}$. The relative magnitudes of these components were determined by holding the incident angle fixed at 60° and measuring the dependence of SHG intensity on incident polarization. The ratio between these two tensor components should be 3.0 in the chromophore−gas description; however, we find $\chi^{(2)}_{zzz}/\chi^{(2)}_{zxx} > 8$. This very large anisotropy is completely inconsistent with the standard model of isolated dipoles interacting with the dc field.[4,32]

SHG measurements on a corona-poled 2% DANS + PMMA sample with $E_p = 10^6$ V cm^{-1} were performed for comparison The film response was found to be optically uniaxial, with the symmetry axis normal to the film (in this case defined as the *x* direction), which is typical of corona-poling experiments on chromophore-doped thin films. The magnitude of $\chi^{(2)}_{xxx}$ was determined to be $\sim 2 \times 10^{-9}$ esu ($\lambda_0 = 1.064$ nm), which is in accord with that expected for a 2% DANS + PMMA sample at this relatively low chromophore number density.[33]

The frequency dependence of the film SHG response for the two poling configurations was next examined, and the results clearly differentiate the in-plane poling case from the corona-poling case. The in-plane responses both parallel to and perpendicular to the poling field direction (Figure 4) exhibit a sharp resonance around the chromophore λ_{max}. In contrast, the corona-poled response (Figure 3) tracks the linear absorption more closely with a broader resonance, and the fwhm increases by factor of 4, more typical of poled polymeric materials.[34] The two in-plane response curves have similar shapes but very different magnitudes, although a second feature located at the SHG wavelength of 475 nm is much more pronounced in the perpendicular response. Importantly, the in-plane polarized SHG data also contain broad features at longer wavelengths (located near 600 and 675−750 nm) and the response remains strong at SHG wavelength as large as 800 nm. Because of experimental limitations, we were unable to accurately measure the in-plane parallel ($\chi^{(2)}_{xxx}$) frequency dependence for wavelengths longer than 600 nm. Over the measured range, the frequency dependence of $\chi^{(2)}_{zzz}$ and $\chi^{(2)}_{xxx}$ is found to be similar. This similarity may arise from a distribution in the alignment of chromophore aggregates (*vide infra*) induced by the in-plane poling electrodes.[35]

Chart 2. Charged DANS Dimer

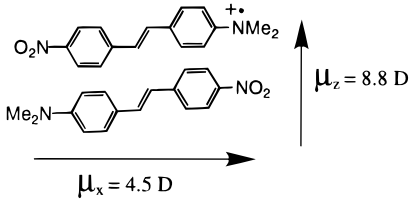

Table 1. ZINDO-Derived Linear Optical Spectroscopic and Second-Order Hyperpolarizability (10^{-30} cm^5 esu^{-1}) Data for DANS Dimers[a]

structure	μ_x (D)	μ_z (D)	λ_{max} (nm)	*f*	β_{xxx} (0.0)
DANS monomer	9.9		383	1.2	43.1
$(DANS)_2$ H-type (**II**)	18.7	0.9	362	2.0	68.1
$(DANS)_2$ J-type (**III**)	18.8	0.9	397	0.3	70.1
			375	0.2	
			357	1.8	
$(DANS)_2^{\bullet+}$ (Chart 2)	4.5	8.8	826	1.5	90.2
			741	0.4	
			715	1.3	
			535	1.1	
			502	0.2	
			471	0.3	
			454	0.2	
			418	0.2	
			384	0.4	
			⋮	⋮	
			339	0.35	
			338	1.01	

[a] **I** will have linear optical features similar to those of **II** but will have $\beta_{xxx} = 0$.

Theoretical Results. Quantum chemical INDO-SOS calculations on the model $(DANS)_2$ and $(DANS)_2^{\bullet+}$ supermolecules (Chart 1) were undertaken to probe the electronic structure and NLO response of neutral and positively charged chromophore aggregates.[36] They indicate the existence of electronic states associated with both symmetric and asymmetric distributions of the positive charge within the $(DANS)_2^{\bullet+}$ dimer. Of course, in the case of a symmetrical charge distribution, a vanishing ground state dipole moment and, hence, a vanishing second-order nonlinearity are calculated. In particular, the removal of one electron from the HOMO of the neutral centrosymmetric $(DANS)_2$ dimer, without any symmetry constraints (broken-symmetry calculations), results in a localized $(DANS)_2^{\bullet+}$ ground state. This state has associated with it charge localization ($\sim$95%) on one DANS unit of the $(DANS)_2^{\bullet+}$ supermolecule. The computed dipole moment of this localized state along the *x* axis is 4.5 D, while along the intermolecular (*z*) axis, it is 8.8 D, a value corresponding to a charge separation of $\sim$1 e.u. between the two DANS units (Chart 2). Moreover, this electronic state possesses various low-energy excited states having charge-transfer (CT) character (Table 1). This set of excited states strongly differs from those originating from centrosymmetric H-type or J-type neutral DANS dimeric aggregates (Chart 1). In fact, while the CT excited states of the neutral dimers can be simply related to those of DANS monomer, blue- or red-shifted due to excitonic, dipolar interac-

(32) (a) Herminghaus, S.; Smith, B. A.; Swalen, J. D. *J. Am. Opt. Soc. B* **1991**, *8*, 2311. (b) Morichère, D.; Chollet, P.-A.; Fleming, W.; Jurich, M.; Smith, B. A.; Swalen, J. D. *J. Am. Opt. Soc. B* **1993**, *10*, 1894.

(33) Page, R. H.; Jurich, M. C.; Reck, B.; Sen, A.; Tweig, R. J.; Swalen, J. D.; Bjoklund, G. C.; Willson, C. G. *J. Opt. Soc. Am. B* **1989**, *7*, 733.

(34) Crumpler, E. T.; Reznichenko, J. L.; Li, D.; Marks, T. J.; Lin, W.; Lundquist, P. M.; Wong, G. K. *Chem. Mater*. **1995**, *7*, 596.

(35) Stahelin, M.; Walsh, C. A.; Burland, D. M.; Miller, R. D.; Twieg, R. J.; Volksen, W. *J. Appl. Phys*. **1993**, *73*, 8471.

(36) The dimer is presumed to be positively charged. This is supported by the present EPR results and previous observations that the nonlinearity initially appears near the positive electrode,[7] which also argues that it is due to hole injection.

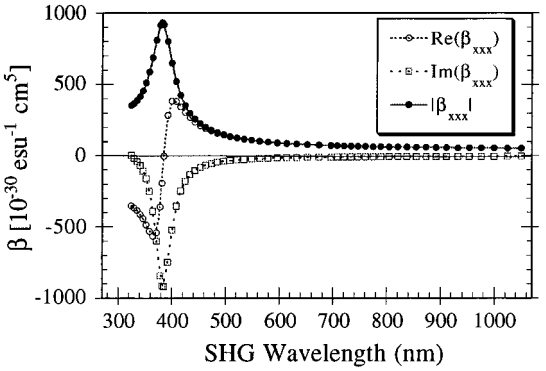

Figure 6. Computed frequency dependence of the real (empty circles) and imaginary (empty squares) components of the largest tensor component of the complex hyperpolarizability, $\beta_{xxx}(-2\omega;\omega,\omega)$, and its modulus $|\beta_{xxx}|$ (filled circles, see eq 4) as a function of the SHG wavelength for the DANS monomer.

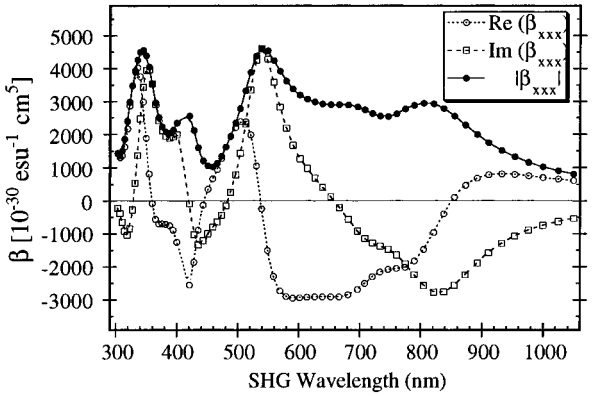

Figure 7. Computed frequency dependence of the real (empty circles) and imaginary (empty squares) components of the largest tensor component of the complex hyperpolarizability, $\beta_{xxx}(-2\omega;\omega,\omega)$, and its modulus $|\beta_{xxx}|$ (filled circles, see eq 4) as a function of the SHG wavelength for the $(DANs)_2^+$ dimer.

tions,[37] in the case of the asymmetric $(DANS)_2^{\bullet+}$ dimer, in addition to monomer-related blue-shifted states, a new set of low-lying excited states is predicted in the region between 450 and 800 nm. These excited states, either excitonic or cross-excitational in character, almost invariably involve the HOMO, representing the partially filled orbital. Moreover, these excitations possess an appreciable intensity ($f = 0.2-1.5$, where f is the calculated oscillator strength) and are accompanied by an appreciable dipole moment change ($\Delta\mu$) mainly along the molecular x axis and, to a minor extent, along the intermolecular z axis. The calculated low-energy electronic transitions of the $(DANS)_2^{\bullet+}$ dimer can be associated with the long-wavelength features observed in the experimental linear absorption spectra of DANS−PMMA films poled in the "in-plane" configuration (Figure 4) and are likely responsible for the large second-order response and the anomalous SHG dispersion observed at longer wavelengths (*vide infra*). Clearly, in this case, the "two-state" approximation is not valid since all these states (instead a single state) contribute to the nonlinearity. Therefore, the two-level ($\beta_{ijk,2}$) sum, i.e., all two-level contributions, in addition to the three-level contributions ($\beta_{ijk,3}$),[17] must be considered to account for the NLO response of $(DANS)_2^{\bullet+}$. The calculated static hyperpolarizability of $(DANS)_2^{\bullet+}$ ($\beta_{xxx} = 90.2 \times 10^{-30}$ cm^5 esu^{-1}) is substantially larger than that of the DANS monomer ($\beta_{xxx} = 43.1 \times 10^{-30}$ cm^5 esu^{-1}), the neutral H-type DANS dimer (structure **II**; $\beta_{xxx} = 68.1 \times 10^{-30}$ cm^5 esu^{-1}) and the neutral J-type dimer (structure **III**; $\beta_{xxx} = 70.1 \times 10^{-30}$ cm^5 esu^{-1}). In all cases, the β_{xxx} term is the principal component of the β_{ijk} tensor and for $(DANS)_2^{\bullet+}$ is aligned *perpendicular* to the largest calculated molecular dipole moment vector (μ_z; Chart 2).

The present semiempirical results are in full agreement with *ab initio* calculations on simpler centrosymmetric dimeric $(PNA)_2^{\bullet+}$ supermolecules[18] in which the most stable state is also associated with an asymmetric charge distribution, and β_{xxx} is also the largest hyperpolarizability tensor component. Moreover, the *ab initio* results indicate that aggregate formation ($PNA + PNA^{\bullet+} \rightarrow (PNA)_2^{\bullet+}$) thermodynamically stabilizes the positive charge and enhances the optical nonlinearity.

Figures 6 and 7 show the evolution of the real and imaginary part of $\beta(-2\omega;\omega,\omega)$ as a function of the SHG wavelength for the largest β_{xxx} tensor of the neutral DANS monomer and of the $(DANS)_2^{\bullet+}$ dimer, respectively. In the case of the DANS monomer (Figure 6), a single resonance occurs at ∼380 nm corresponding to the calculated λ_{max} value, as expected. In contrast, the β_{xxx} tensor of the $(DANS)_2^{\bullet+}$ dimer exhibits a strong calculated resonance at ∼340 nm (corresponding to that of the monomer but slightly blue-shifted), at ∼420 nm, and in the region between 530 and 830 nm (Figure 7). Moreover, at all frequencies investigated, the $Re(\beta_{xxx})$ tensor is about 1 order of magnitude larger than that of the DANS monomer. The $Im(\beta_{xxx})$ tensor, which arises from the damping term, is also very large at all frequencies. These results are in reasonable agreement with the observed anomalous perpendicular dispersion in the higher wavelength region of the in-plane poled DANS polymer films, although full comparison between the theoretical calculated $|\beta_{xxx}|$ value and the experimental $\chi^{(2)}_{zzz}$ data requires more exact information about structure of the charged aggregate (we have pragmatically assumed the simplest dimeric species; however, larger aggregates cannot be excluded) and the inclusion of effects due to the matrix[24] and counteranion.[38] Both effects are expected to shift the calculated λ_{max} values and, in turn, the SHG resonance. Therefore, the present calculated dispersion data do not allow assessment as to whether the stronger dispersion feature observed at ∼430 nm is related to the calculated resonance at ∼550 nm or that at ∼340 nm or to a superposition of both.

Discussion

The present linear and nonlinear optical as well as EPR results on DANS−polymer films poled in an "in-plane" configuration are all consistent with the existence of charged DANS aggregates. In particular, the observed differences in the linear optical properties of in-plane and corona-poled samples—the former exhibiting a broader absorption band tailing to the red and bathochromically shifted emission—suggest the creation of charged DANS aggregate species via the in-plane poling. EPR measurements in addition support the formation of charged, open-shell DANS species. Furthermore, the computational results predict that aggregate formation stabilizes[18] the DANS-centered positive charge and enhances the nonlinearity.

Figure 8 summarizes the proposed scheme for charge injection in the in-plane poling geometry for DANS dissolved in PMMA. Oxidation of the DANS amino group via hole injection (h^+) is coupled to reduction of the ester group in PMMA by electron injection. The oxidized, radical cation product is detected by EPR. No direct evidence is found for PMMA-derived acyl radicals. However, mechanisms are known in the literature for the dimerization of acyl radicals[31] in PMMA mainly via an

(37) Di Bella, S.; Ratner, M. A.; Marks, T. J. *J. Am. Chem. Soc.* **1992**, *114*, 5842.

(38) Di Bella, S.; Fragalà, I.; Ratner, M. A.; Marks, T. J. *Chem. Mater.* **1995**, *7*, 400.

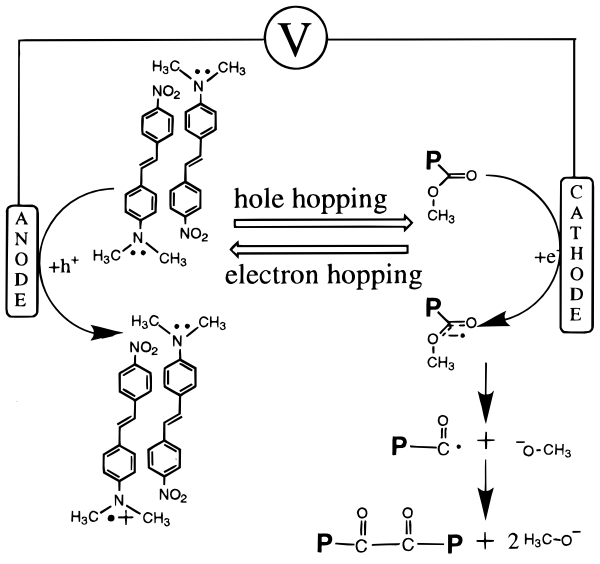

Figure 8. Proposed chemical/electrochemical reaction scheme for DANS dispersed in a PMMA matrix under charge injection conditions during in-plane poling.

acyloin ester condensation[39] mechanism. Such a process will consume the acyl radicals, producing low molecular weight methoxide ions that will presumably diffuse away and ultimately stabilize the cation−radical dimer. This scenario can explain why only chromophore-derived radicals are detected and not those from the PMMA matrix. Electrochemical studies on DANS[40] revealed that this dye undergoes one-electron reduction as well as one-electron oxidation processes, each characterized by a first reversible redox wave and a second irreversible redox wave. This behavior was attributed to the formation of stable mono-charged dimeric species (anionic or cationic, respectively).[40] The electrochemical formation of a very stable radical cations has also been observed for other *p*-(dimethylamino)-stilbene derivatives.[41]

The present NLO data indicate a polar ordering in the direction of the surface normal and that the anomalous SHG response has a frequency dependence quite distict from the isolated chromophore response. Neither the orientation nor the extremely large magnitude of the SHG response of in-plane poled thin films can be explained by the electric field-induced alignment of isolated chromophores. Even perfect alignment of every chromophore molecule is insufficient at the present chomophore number densities to cause electric-dipole related NLO effects of this magnitude. Qualitatively, the in-plane poled samples possess the features predicted for a radical−cation DANS dimer. In fact, the INDO-SOS computations on a positively charged DANS dimer (localized hole state) predict an extremely large response over a broad range of frequencies ($|\beta_{xxx}| = (1000-5000) \times 10^{-30}$ cm^5 esu^{-1}), even at relatively long wavelengths (~840 nm). The response is predicted to be about one order of magnitude larger than that of the isolated DANS chromophore (Figures 6 and 7). This model can account for the anomalously large NLO response observed after poling and subsequent charge injection and trapping. Moreover, the theoretical results predict approximate orthogonality of μ and β with the principal molecular dipole moment oriented along the dimer intermolecular axis and the largest hyperpolarizability tensor term oriented along the dimer long axis, thus implicating

Scheme 1

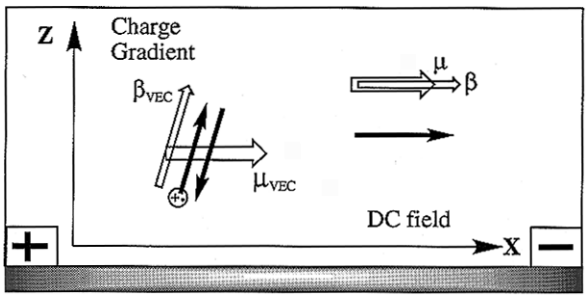

an "*intramolecular*" mechanism as dominating the optical nonlinearity of $(DANS)_2^{\bullet+}$. The enhancement of the nonlinearity in the longer wavelength region is due to the presence of various low-lying CT states, absent in the neutral monomer or dimer aggregates. These states can account for the low-intensity, longer wavelength features observed in the linear absorption spectra of the in-plane poled DANS−PMMA samples. It is worth mentioning that the $\chi^{(3)}$ response of poly(bithiophene) was recently observed to be enhanced by one order of magnitude upon electrochemical creation of radical cation states.[42]

The combination of the previous results with the current ones allows us to suggest a model (Scheme 1) for the anomalously strong nonlinearity observed for in-plane poled chromophore−glassy polymer films. In this model, the dc field aligns the neutral species (monomers and other acentric species) in the *x* direction, thus producing some bulk second-order nonlinearity parallel to the field (μ and β are parallel). In the case of charged dimers and other aggregates, the electrostatic field aligns the charged dimers with the intermolecular stacking axes (the principal μ direction) predominantly parallel to the field and the principal β direction normal to the field. However, this orthogonality of μ and β alone cannot explain these anomalous SHG responses since only a preferential charge trapping along the *z* direction will lead to a net nonlinearity perpendicular to the dc field. Aluminum ($\phi = 4.19$ eV) can readily provide electrons for charge injection. Charge injected into the film from these low-work-function Al electrodes first accumulates at the substrate/polymer interface before diffusing toward the polymer/air interface. The directional charge migration leads to charge gradients within the polymer film, directed along the surface normal. The gradients in this direction are caused by the relative thinness of the electrodes, and the diffusion is governed by electric field drift mobility. The diffusion of charges in a specific direction (+*z*) could lead to a preferential aggregate charge trapping site location (e.g., localized trapped charges on NMe_2 groups nearest the substrate), thus leading to broken symmetry in the surface normal direction. Such a process would impose an average orientation of the charged dimer principal β direction along the film surface normal (Scheme 1).[43] The charged dimer/polar alignment is subsequently stabilized by the dc field due to the orthogonality of μ and β.

Conclusions

The present EPR, linear, and nonlinear optical spectroscopy, as well as INDO/SOS calculations provide strong support that the anomalous SHG response observed in DANS-doped polymer

(39) Bloomfield, J. J.; Owesly, D. C.; Nelke, J. M. *Org. React.* **1976**, *23*, 259.

(40) Todres, Z. V.; Ermekov, D. S.; Rakhimov, R. D.; Zhil'tsov, V. V.; Kazakova, V. M. *Metalloorg. Khim.* **1992**, *5*, 1207.

(41) Bard, A. J.; Phelps, J. *J. Electroanal. Chem.* **1970**, *25*, App. 2.

(42) Meerholtz, K.; Swiatkiewicz, J.; Prasad, P. N. *J. Phys. Chem.* **1995**, *99*, 7715.

(43) It is also possible that the response is due at least in part to electric quadrupole moment SHG mechanisms,[2] which are typically negligible, because the electric quadrupole moment of a symmetric dimer is the lowest order term in the multipole expansion. If this is the case, the charge injection evidence would still indicate that the response is related to charge injection and trapping onto the dimers.

films poled in an "in-plane" configuration is related to the formation of charged chromophore aggregates. Moreover, the present data support a new model for explaining the large optical nonlinearity of such systems. These findings have two major scientific and technological implications: (a) a new approach to maximizing second-order NLO responses and (b) possible explanation for the large, long wavelength optical losses observed in many poled polymeric NLO waveguiding devices.[44] The first implementation of these results would be to devise ways to produce charged aggregates and to design a proper matrix to stabilize them. The second ramification is a proposed interpretation and solution to the large optical losses currently observed in pole polymeric NLO devices. The present results suggest that these losses can originate from similar "electro-oxidative" mechanisms. Thus, proper buffer layers and anti-oxidants should be developed and incorporated into poled polymeric waveguiding devices.

(44) (a) Teng, C. C.; Mortazavi, M. A.; Boudoughian, G. K. *Appl. Phys. Lett.* **1995**, *66*, 667. (b) Kowalczyk, T. C.; Kosc, T.; Singer, K. D.; Cahill, P. A.; Seager, C. H.; Meinhardt, M. B.; Beuhler, A. J.; Wargowski, D. A. *J. Appl. Phys.* **1994**, *76*, 2505. (c) Skumanich, A.; Jurich, M.; Swalen, J. D. *Appl. Phys. Lett.* **1993**, *62*, 446.

Acknowledgment. We acknowledge the NSF-MRL Program (Grant DMR 9120521) through the Northwestern University Materials Research Center and AFOSR (Contract 94-0169) for support of this research. S.D.B. thanks the Consiglio Nazionale delle Ricerche (CNR, Rome) and the MURSR (Rome) for financial support. We thank Dr. P. E. Doan for his assistance with the EPR measurements.

JA963489Y